TEMPORAL EVOLUTION OF PHYSICAL PARAMETERS IN GRANULE

J. Koza[1], L.R. Bellot Rubio[3], A. Kučera[1], A. Hanslmeier[2], J. Rybák[1], and H. Wöhl[3]

[1]Astronomical Institute of the Slovak Academy of Sciences, SK-05960 Tatranská Lomnica, Slovak Republic
[2]Institut für Geophysik, Astrophysik und Meteorologie, Universitätsplatz 5, A-8010 Graz, Austria
[3]Kiepenheuer-Institut für Sonnenphysik, Schöneckstr. 6, D-79104 Freiburg, Germany

ABSTRACT

The temporal evolution of the physical parameters inside a granule is presented. This is a step towards a more realistic 1D modeling of the solar granulation, avoiding the temporal averaging used up to now. The granulation is treated as a dynamical phenomenon and our model has been calculated using an inversion method applied to time series of spectra. The granular evolutionary model is presented in the form of the functional dependence of temperature $T(\log\tau, t)$ and line-of-sight velocity $v_{LOS}(\log\tau, t)$ on optical depth τ and time t. The observed disappearance of the granule is accompanied with significant temperature changes greater than $\sim 300\,\mathrm{K}$ in deeper layers ($\log\tau_5 > 0$) and upper layers ($\log\tau_5 < -2.5$). In contrary, the layers from $\log\tau_5 \simeq -0.5$ to $\log\tau_5 \simeq -1.5$ are more stable in the sense of temperature variations, which are less then $\sim 150\,\mathrm{K}$. An oscillatory behavior is found in the line-of-sight velocity stratification from $\log\tau_5 \simeq 0$ upwards with increasing amplitude reaching up to $\simeq 2\,\mathrm{km\,s^{-1}}$ in upper layers.

Key words: Sun: granulation – Sun: photosphere – stars: atmospheres – line: profiles.

1. INTRODUCTION

The principal physical process taking place in layers near the surface of the Sun is the intensive radiative cooling of the ascending plasma. As a direct consequence, larger convective upflows are smashed giving rise to the granulation with seemingly dominant laminar behavior along with properties suggesting turbulence [10]. Due to the inertia, the granules penetrate into the stable photospheric layers overshooting their nearly-parallel structure and thus disturb the hydrostatic equilibrium. This process is accompanied with a transformation of the energy carried by the granule into the radiation, waves and shocks. To understand such conversion, it is necessary to know the temporal and spatial gradients of the fundamental physical quantities in granular interior as well as overlying photosphere on scales substantially smaller than the dimension and lifetime of the granule. Presently, there are two approaches to accomplish that. During the last two decades, theoretical simulations based on the equations of hydrodynamics succeeded to explain many details of granular structure [1], [3]. Another approach is based on modeling of the photospheric line profiles observed with high spectral, spatial and temporal resolution. For this and many other purposes a powerful inversion method was developed [14]. In the present paper we use this inversion technique [13] to study the temporal evolution and radial stratification of the temperature and line-of-sight velocity in granular photosphere.

2. OBSERVATIONAL DATA

The spectra obtained as time series with the Echelle spectrograph of the German VTT, Tenerife, on June 1, 1993, are used as input observational data. The time series consists of 28 pairs of spectra of spectral regions around 522.5 nm and 557.6 nm. The profiles of two medium strong Fe I 522.5 nm and 557.6 nm lines and one weak Fe I 557.7 nm line have been selected. The time step between exposures of subsequent pairs was 9 s and the whole time series covers 4 min of the decay of a granule. The spatial resolution along the slit was 0.175" per pixel and the width of the spectrograph slit was 150 μm. The exposure time was 0.2 s. We identified the bright granule by visual inspection of individual spectra at position 5 arcsec (see Fig.1), whose disappearance has been possibly related with the extinction. For further investigation, the Fe I line profiles were used from the center of the selected granule. Because the spectra lack an absolute wavelength calibration, the wavelength scale was assigned using the pairs of suitable lines as standards with the solar wavelengths known accurately from an FTS atlas [12]. The pairs Ti I 522.49 nm – Fe I 522.53 nm and Fe I 557.6 nm – Fe I 557.7 nm were adopted in relevant spectral ranges.

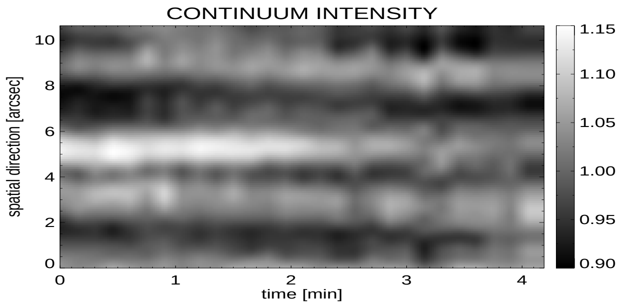

Figure 1. Time-slice map of the continuum intensity in 522.5 nm spectrum along the slit demonstrating the evolution of the granule under study at slit position $\simeq 5$ arcsec.

3. THE METHOD OF THE SPECTRAL INVERSION

The observed spectra are inverted with the help of the SIR code (**S**tokes **I**nversion based on **R**espons functions). SIR iteratively modifies an initial guess model until the synthetic spectrum matches the observed one. The squared differences χ^2 between observed and synthetic spectrum are calculated in each iteration step providing a feedback information how to modify the guess model, which should lead to minimization of χ^2 in the next iteration. The code was prepared to deal with the four Stokes line profiles, but we analyze Stokes I profiles only. The basic assumptions are LTE, homogeneous plan-parallel atmosphere and hydrostatic equilibrium. As a result of the inversion, SIR provides the stratification with optical depth τ of temperature T, line-of-sight velocity v_{LOS} and microturbulence v_{MIC} along the whole atmosphere. It also returns the macroturbulenece v_{MAC} which is assumed to be hight-independent. The application of the SIR code to the time series of the spectra can provide the time dependence of these parameters. The latest SIR version presented in [5] makes use of a quantum mechanical formulation of the collisional broadening [4] as well as classical Unsöld's formula, which can be modified by means of an enhancement factor. The atomic parameters of the atomic transitions considered are sumarized in Tab.1. The central laboratory wavelengths in air have been taken from [11] except for the 557.7 nm line (see below). The excitation potential of the lower level and the logarithm of the oscillator strength have been adopted from [16]. The temperature parameter and cross section needed for collisional broadening calcuations have been taken from [4]. In the case of the weak 557.7 nm line, the Unsöld's theory is considered to be sufficient and the enhancement factor has been set to 1. We adopt an iron abundance of 7.46 dex. This value is appropriate for LTE calculation according to [2], [15]. In addition to the atomic parameters, the inversion code requires an initial guess model. We have chosen the Harvard-Smithsonian Reference Atmosphere (HSRA) [6]. The microturbulence and line-of-sight velocity were set to $0.6\,\mathrm{km\,s^{-1}}$ in all optical depths and the macroturbulence was $2\,\mathrm{km\,s^{-1}}$. The profiles of the Fe I 522.5 nm, 557.6 nm and 557.7 nm lines were sampled at intervals of 0.35 pm, 0.39 pm and 0.39 pm respectively. The red wings of the Fe I 522.5 nm and 557.6 nm were excluded from inversion because of blending. The weak 557.7 nm lacks part of the red wing because it was already outside of the CCD chip. Thus, 168 data points from each spectrum have been used for the inversion.

Table 1. Fe I line atomic parameters. λ_{lab}^{air} indicates the central laboratory wavelength in air, EP_{low} the excitation potential of the lower level, and log(gf) the logarithm of the oscillator strength times the multiplicity of the lower level. α and σ stands for temperature parameter and cross section, a_0 is Bohr radius.

λ_{lab}^{air} [nm]	EP_{low} [eV]	log(gf)	α	σ [a_0^2]
522.55261	0.11	-4.74	0.253	207
557.60888	3.43	-0.73	0.232	854
557.70248	5.03	-1.53	–	–

4. THE PROBLEM OF THE 557.7 NM LINE IDENTIFICATION

The weak 557.7 nm line has not yet been observed in any laboratory spectra and thus it is not listed in [11]. The line identification in [8] as neutral iron line has been based upon coincidence of the wavelength predicted from less precise energy levels and a feature in the solar solar spectrum. To obtain the accurate laboratory wavelength in air and to test the identification, we apply the following procedure. Knowing the multiplet number [8] and designation [9], we can determine from [11] the wavenumbers of the lower and upper level of the transition needed for the calculation of the laboratory wavelength in air [11]. Using this value, the two-component model of the solar photosphere [5] and the SIR code, we calculated the synthetic 557.7 nm line profile, provided it is an iron line. The agreement of the synthetic profile central wavelength 557.70249 nm with the central wavelength 557.70247 nm of the profile extracted from FTS atlas proves convincingly the identification.

5. RESULTS OF THE INVERSION

The profiles of all three Fe I lines were inverted simultaneously in three cycles allowing one, four and five nodes for temperature and line-of-sight velocity. The micro- and macroturbulence were assigned with one node. In very few cases, to achieve a satisfactory agreement between synthetic and observed profiles, six or seven nodes were used for temperature in the last cycle. As an example, we plot in Fig.2 the observed profiles at $t = 0$ min and the synthetic profiles

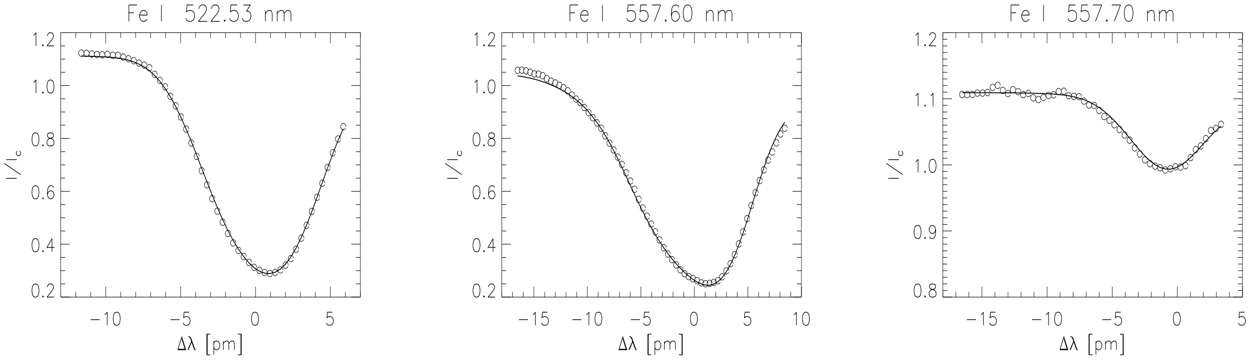

Figure 2. Observed profiles (circles) at t = 0 min and synthetic profiles (solid) resulting from the inversion. The label 0 pm corresponds to the central laboratory wavelength. The gravitational redshift has not been subtracted.

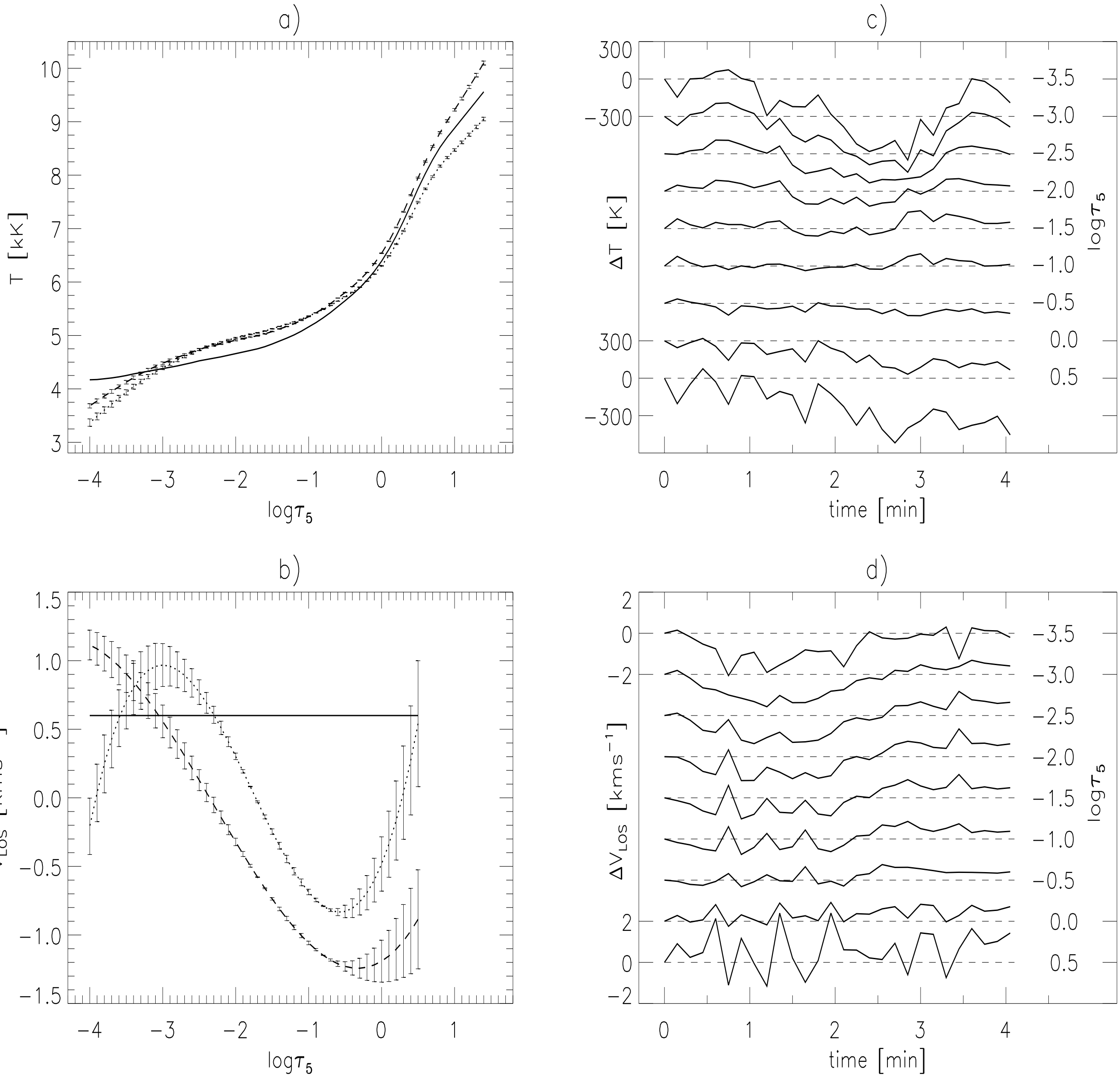

Figure 3. The temperature and line-of-sight velocity stratifications in the granular photosphere at t = 0 min (dashed line) and t = 4 min (dotted line). The initial guess model (solid line) is depicted without errorbars. Negative velocities indicate upflows. The velocity has been corrected for gravitational redshift by subtracting 636 m s^{-1} **(a), (b)**. *The temporal evolution of the temperature and line-of-sight velocity differences (solid line) with respect to the first model at t = 0 min (horizontal dashed lines) at indicated optical depths. For clarity, the curves have been shifted by $\Delta T = 300\,K$ and $\Delta v_{LOS} = 2\,km\,s^{-1}$* **(c), (d)**.

resulting from the inversion. In general, SIR succeeded very well in reproducing of the line cores of the whole series. Discrepancies with maximum relative errors of up to 4 % appeared sometimes in the blue wing of the Fe I 557.6 nm line. Figs.3a and 3b show the models determined from the inversion at t =0 min and 4 min. The errors in the temperature stratifications of all 28 inferred models are smaller than ± 60 K at all optical depths. In these figures, we also depict the initial guess model without errorbars. Figs.3c and 3d represent the temporal evolution of the temperature and line-of-sight velocity differences with respect to the first model at t =0 min.

6. DISCUSSION

The layers from $\log\tau_5 = 0.5$ to $\log\tau_5 = -3.5$ are discussed only, because the temperature response function is significantly greater than zero for these layers, what is highly important with regard to the inversion method used [13]. The temporal evolution of the temperature stratification $T(\log\tau, t)$ shown in Fig.3c exhibits non-uniform response of the granular photosphere during the decay of the bright granule. Whereas deeper layers ($\log\tau_5 > 0$) exhibit systematic cooling with temperature decrease greater than ~ 300 K, the low and middle photosphere from $\log\tau_5 \simeq -0.5$ to $\log\tau_5 \simeq -1.5$ exhibit certain temperature stability with temperature changes less than ~ 150 K. On the contrary, more pronounced temperature changes greater than ~ 300 K occur again in upper layers ($\log\tau_5 < -2.5$) probably phase shifted with respect to changes taking place in deeper layers. There exists noticeable rise of temperature of upper layers ($\log\tau_5 < -1$) between third and fourth minute, when the granular evolution is close to the final stage. Comparable results were obtained in HD simulations of the relative temperature fluctuations in the granular photosphere (Fig.5 in [3]). The models of the velocity stratification at t =0 min and 4 min in Fig.3b posses zero crossing points, in which the line-of-sight velocities change sign from upflow (negative v_{LOS}) to downflow (positive v_{LOS}). This apparently strange behavior of the granular velocity field is fully testified both theoretically by HD simulations (Fig.2 in [3]) as well as observationally as the anticorrelation between the vertical velocities and temperature fluctuations in the upper photosphere [3]. The layers where the crossing points occur may be considered as boundaries above which mainly non-convective, so called secondary motions plus oscillations predominate [7]. Although in [5] a similar trend was found, the velocity models found here are probably not realistic from $\log\tau_5 \simeq 0$ downwards. The velocity increase towards positive values may be an artefact of the inversion reflecting the lack of direct observational data from deeper layers, for which the velocity response function is close to zero. The temporal evolution of the velocity stratification $v_{LOS}(\log\tau, t)$ shown in Fig.3d exhibits apparent oscillatory behavior from $\log\tau_5 \simeq 0$ upwards with increasing amplitude reaching up to $\simeq 2\,\mathrm{km\,s^{-1}}$ in upper photosphere. This characteristics expresses the contamination of the observational data with 5-min oscillations. To obtain the actual granular velocity field free of oscillations it is necessary to apply spatio-temporal filtering on time series considerably longer than the present one. This is the main aim of our future work.

ACKNOWLEDGMENTS

The Vacuum Tower Telescope is operated by the Kiepenheuer-Institut für Sonnenphysik, Freiburg at the Observatório del Teide of the Instituto de Astrofísica de Canarias. J.K. is very grateful to IAC for substantial support provided in summer 2001 as well as to C.Allende Prieto for kindly providing of the IDL routine mideshift_xy.pro. A.H. thanks the 'Austrian Fonds zur Förderung der wissenschaflichen Forschung' for support. A.H., A.K and J.R. acknowledge the Austrian and Slovak Academies of Sciences, J.K., A.K. and J.R. acknowledge the Grant VEGA 2/7229/20 and A.K., J.R. and H.W. acknowledge the German DFG grant 436 SLK 113/7/0-1.

REFERENCES

1. Asplund, M., Nordlund, A., Trampedach, R., Allende Prieto, C., Stein, R.F.: 2000, A&A, 359, 729

2. Asplund, M., Nordlund, A., Trampedach, R., Stein, R.F.: 2000, A&A, 359, 743

3. Atroshchenko, I.N., Gadun, A.S.: 1994, A&A, 635, 1994

4. Barklem, P.S., Piskunov, N., O'Mara, B.J.: 2000, A&AS, 142, 467

5. Borrero, J.M., Bellot Rubio, L.R.: 2002, A&A, 385, 1056

6. Gingerich, O., Noyes, R.W., Kalkofen, W., Cuny, Y.: 1971, Sol.Phys., 18, 347

7. Hanslmeier, A., Kučera, A., Rybák, J., Neunteufel, B., Wöhl, H.: 2000, A&A, 356, 308

8. Moore, C.E., Minnaert, M.G.J., Houtgast, J.: 1966, The Solar Spectrum 2935 Å to 8770 Å, NBS Monograph 61, Washington: USGPO

9. Moore, C.E.: 1972, A Multiplet Table of Astrophysical Interest, NSRDS-NBS 40, Washington

10. Muller, R.: 1999, in Motions in the Solar Atmosphere, eds: Hanslmeier, A., Messerotti, M., Kluwer Academic Publishers, Dordrecht, 35

11. Nave, G., Johansson, S., Learner, R.C.M., Thorne, A.P., Brault, J.W.: 1994, ApJS, 94, 221

12. Neckel, H.: 1999, Sol.Phys., 184, 421

13. Ruiz Cobo, B., del Toro Iniesta, J.C.: 1992, ApJ, 398, 375

14. Ruiz Cobo, B.: 1998, Ap&SS, 263, 331

15. Shchukina, N., Trujillo Bueno, J.: 2001, ApJ, 550, 970

16. Thévenin, F.: 1989, A&AS, 77, 137